

STUDENT SUMMER INTERNSHIP TECHNICAL REPORT

Radial Jet Impingement Correlation Investigation

DOE-FIU SCIENCE & TECHNOLOGY WORKFORCE DEVELOPMENT PROGRAM

Date submitted:

September 30, 2015

Principal Investigators:

Maximiliano Edrei (DOE Fellow Student)
Florida International University

Chris Guenther (Mentor)
National Energy Technology Laboratory

Rahul Garg (Mentor)
AECOM

Florida International University Program Director:

Leonel Lagos Ph.D., PMP®

Submitted to:

U.S. Department of Energy
Office of Environmental Management
Under Cooperative Agreement # DE-EM0000598



Applied Research Center

FLORIDA INTERNATIONAL UNIVERSITY

DISCLAIMER

This report was prepared as an account of work sponsored by an agency of the United States government. Neither the United States government nor any agency thereof, nor any of their employees, nor any of its contractors, subcontractors, nor their employees makes any warranty, express or implied, or assumes any legal liability or responsibility for the accuracy, completeness, or usefulness of any information, apparatus, product, or process disclosed, or represents that its use would not infringe upon privately owned rights. Reference herein to any specific commercial product, process, or service by trade name, trademark, manufacturer, or otherwise does not necessarily constitute or imply its endorsement, recommendation, or favoring by the United States government or any other agency thereof. The views and opinions of authors expressed herein do not necessarily state or reflect those of the United States government or any agency thereof.

ABSTRACT

Provide analytical work to support the investigation of the use of PJM vessels at Hanford Waste Treatment Facility (WTP) which leverages previous work found in the literature. One example is the paper Investigation of a turbulent radial wall jet (Poreh et al,1967) that studied the radial wall jets produced from impingement of turbulent round jets. Based on their detailed experiments, Poreh et al. proposed correlations for maximum jet velocity and radial wall jet thickness. The correlations are based off a non-dimensional number that takes into account the ratio of the initial jet diameter and the distance from the nozzle to the impingement surface. There has been skepticism on the use of these correlations due to the fact that the actual ratio in the PJMs is much smaller than the one tested in the paper. In this study, the correlations obtained from Poreh's paper are validated for the characteristic non-dimensional values observed in the PJMs through Star-CCM+ computational fluid dynamics (CFD) modeling software using RANS based turbulence modeling. The results show that the maximum velocity correlations hold reasonably well for the PJM application. The second correlation is seen to have a weaker agreement but is still within a reasonable range.

TABLE OF CONTENTS

| | |
|------------------------------|-----|
| ABSTRACT..... | iii |
| TABLE OF CONTENTS..... | iv |
| LIST OF FIGURES | v |
| LIST OF TABLES | v |
| LIST OF EQUATIONS | v |
| 1. INTRODUCTION | 1 |
| 2. EXECUTIVE SUMMARY | 2 |
| 3. RESEARCH DESCRIPTION..... | 3 |
| 4. SET UP & METHODS..... | 6 |
| 5. RESULTS AND ANALYSIS..... | 15 |
| 6. CONCLUSION..... | 21 |
| 7. REFERENCES | 22 |

LIST OF FIGURES

| | |
|--|----|
| Figure 1. Schematic description of impinging and radial wall jets..... | 3 |
| Figure 2. Correlation graphical description. | 4 |
| Figure 3. Full simulation domain & boundary conditions..... | 6 |
| Figure 4. Jet zones (Poreh et al.)..... | 9 |
| Figure 5. Final mesh. | 9 |
| Figure 6. Round jet velocity profile (24 inches away from the nozzle). | 11 |
| Figure 7. Radial wall jet profile (24 inches away from the axis of symmetry). | 11 |
| Figure 8. Residuals for StarCCM+ $b/D=12$ | 12 |
| Figure 9. Velocity profile of the entire domain ($b/D=12$). | 12 |
| Figure 10. Non-dimensional comparison of at $r=24$ in. ($b/D=12$). | 13 |
| Figure 11. Non-dimensional comparison of at $r=36$ in. ($b/D=12$). | 13 |
| Figure 12. Non-dimensional comparison of at $r=48$ in. ($b/D=12$). | 14 |
| Figure 13. Non-dimensional comparison of at $r=60$ in. ($b/D=12$). | 14 |
| Figure 14. Domain velocity profile for $b/D=1.5$ | 15 |
| Figure 15. Velocity profile prior to impingement..... | 15 |
| Figure 16. Mesh sensitivity for radial wall jet $b/D=1.5$ | 16 |
| Figure 17. Mesh sensitivity pre-impingement. | 17 |
| Figure 18. Non-dimensional maximum velocity comparison..... | 18 |
| Figure 19. Close up of non-dimensional comparison. | 19 |
| Figure 20. Non-dimensional δ correlation comparison. | 19 |

LIST OF TABLES

| | |
|---|----|
| Table 1. Poreh's b/D Testing Ratios | 4 |
| Table 2. Physics Modeling Summary | 8 |
| Table 3. Mesh Summary | 10 |

LIST OF EQUATIONS

| | |
|---|---|
| Equation 1. Characteristic Thickness..... | 3 |
| Equation 2. Maximum Velocity..... | 3 |
| Equation 3. Porehs Kinematic Flux Definition..... | 7 |
| Equation 4. Inlet Intensity for Turbulent Pipe Flow | 7 |

1. INTRODUCTION

Currently, there are 53 million gallons of high level waste (HLW) being stored inside tanks located at the Hanford Site. The Department of Energy's (DOE) main objective is to immobilize the waste in order to prevent contamination to the environment. The planned solution for this objective is to have the radioactive waste undergo separation and vitrification, which converts the waste into glass for permanent storage. The waste needs to have particular rheological properties before it goes through this process, including density, viscosity, porosity, etc. The density of HLW is not homogeneous. The HLW separates itself into multiple layers, referred to as the salt cake, the supernate, and the sludge due to density differences. This gives rise for the need to properly mix the HLW inside the storage tanks prior to treatment.

Pulse jet mixing (PJM) is the method that was chosen by DOE to mix the HLW slurry before the vitrification process. This method involves sucking a portion of the waste in the tank into a pressurized vessel and then injecting it back into the tank in order to mix the waste using the pressurized jets. This process is repeated over a number of cycles. The main reason for choosing PJMs for this task is that there are no mechanical moving parts and the process can be operated remotely with minimal interference required by the workers [1].

Correlations developed by Poreh predict two characteristic velocity profile values after jet impingement. They describe the maximum velocity and the thickness of the radial jet. These two characteristic values can be attained at different radial locations along the radial wall jet.

Poreh's experiment studies the situation where a round jet of air is impinged on a flat perpendicular surface. The correlations are based off a non-dimensional number that takes into account the ratio of the initial jet diameter and the distance from the nozzle to the impingement surface. However, the non-dimensional characteristic ratio that pertains to the PJMs is much smaller than the one tested by Poreh. How well the correlation maintains accuracy with the characteristic ratio that pertains to PJMs will be analyzed. This paper will attempt to shed light on this topic using computational fluid dynamic (CFD) simulations.

2. EXECUTIVE SUMMARY

This research work has been supported by the DOE-FIU Science & Technology Workforce Initiative, an innovative program developed by the US Department of Energy's Environmental Management (DOE-EM) and Florida International University's Applied Research Center (FIU-ARC). During the summer of 2015, a DOE Fellow intern (Maximiliano Edrei) spent 10 weeks doing a summer internship at the National Energy Technology Laboratory in Morgantown under the supervision and guidance of the Director of Computational Science & Engineering Division, Chris Guenther. The intern's project was initiated on June 1, 2015, and continued through August 7, 2015 with the objective of providing insight on the applicability of current radial wall jet correlations used in PJM analysis.

3. RESEARCH DESCRIPTION

In order to begin to assess the correlations developed by Poreh, it is necessary to understand the general physical phenomena that Poreh was investigating in his paper published in 1967. Below is a figure from the paper, graphically outlining and explaining the physical characteristics of jet impingement.

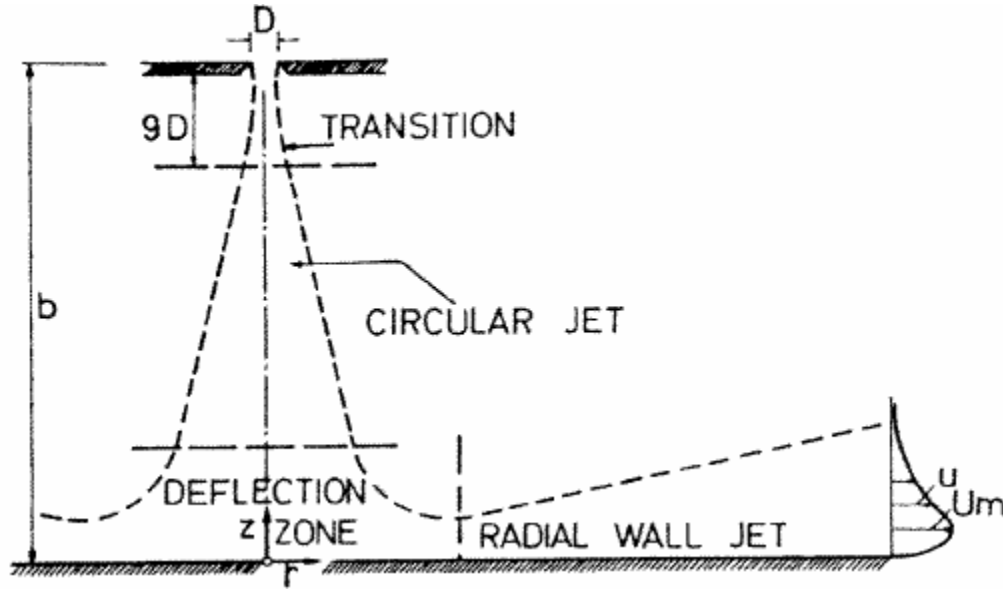


Figure 1. Schematic description of impinging and radial wall jets.

Initially, a round jet is produced at the orifice with diameter D . This round jet velocity profile expands due to shear by surrounding stagnant fluid. The fully developed round jet then impinges a flat surface after a distance b , and produces a radial wall jet. Poreh shows that the velocity profile at the radial wall jet is self-similar as it travels out radially from the center of impingement and therefore asserts a correlation that can describe the velocity profile at any radial distance.

The two correlations developed in Poreh's paper are defined as follows:

$$\delta = b * .098 * \left(\frac{r}{b}\right)^{-0.9}$$

Equation 1. Characteristic Thickness

$$U_m = \frac{\sqrt[2]{K}}{b} * 1.32 \left(\frac{r}{b}\right)^{-1.1}$$

Equation 2. Maximum Velocity

Where:

b = Distance from nozzle to impingement plate

r = Radial distance from impingement center

K = Momentum flux

U_m is the maximum velocity that is reached in the radial wall jet velocity profile, seen in Figure 1. The term δ is defined as the distance (z axis from Figure 1) from the flat surface at which the velocity is half of the maximum velocity. These two terms characterize the velocity profile at each radial location (r). The figure below graphically illustrates these two terms:

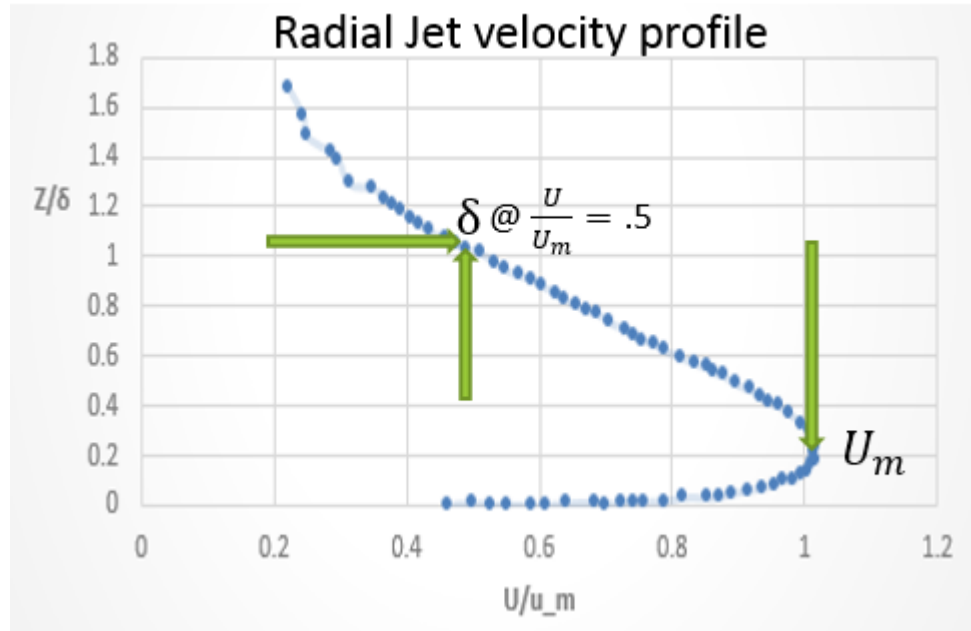


Figure 2. Correlation graphical description.

Poreh's paper obtains these correlations by running the same impinging jet experiments with different Reynolds numbers and b/D ratios. In his experiment, the distance from the nozzle to the impingement surface (b) is held constant at 24 inches. The ratios are changed by altering the orifice diameter. The following table summarizes the b/D ratios that were used in Poreh's experiment:

Table 1. Poreh's b/D Testing Ratios

| Orifice Diameter (inch) | b/D |
|-------------------------|-------|
| 1 | 24 |
| 2 | 12 |
| 3 | 8 |

It is noticed that Poreh only ran experiments down to a b/D of 8. The ratio seen in a typical PJM vessel is 1.5. The round jet is known to be fully developed by the time it hits the impingement plate for such high b/D ratios that Poreh considered. For $b/D=1.5$, however, the round jet will more closely resemble a plug flow before impingement. Because of this fact, it is reasonable to question the applicability of this correlation to PJM vessels and is the motivation for this work.

The approach used in this research replicated one of the experiments ran by Poreh (1967). Once simulations concur with the experimental results the b/D ratio in the simulation was lowered to 1.5 while holding everything else constant. The results were then compared with each other in order to ascertain whether the radial wall jet correlations still apply to a b/D ratio of 1.5.

4. SET UP & METHODS

In order to execute the CFD simulation, information regarding the following sequence of topics was ascertained: Geometry, Boundary Conditions, Physics Models, and Meshing.

4.1 Geometry & Boundary Conditions

The following conditions were used for CFD

1. Half a cylinder domain was created with a radius of 64 inches
2. Orifice was B=2 ft away from the plate
3. 1 inch radius
4. 2 dimensional

The half cylinder domain and 2 dimensionality aspect of the simulation are justified by the axis-symmetric nature of the problem. The following figure shows the resulting geometry.

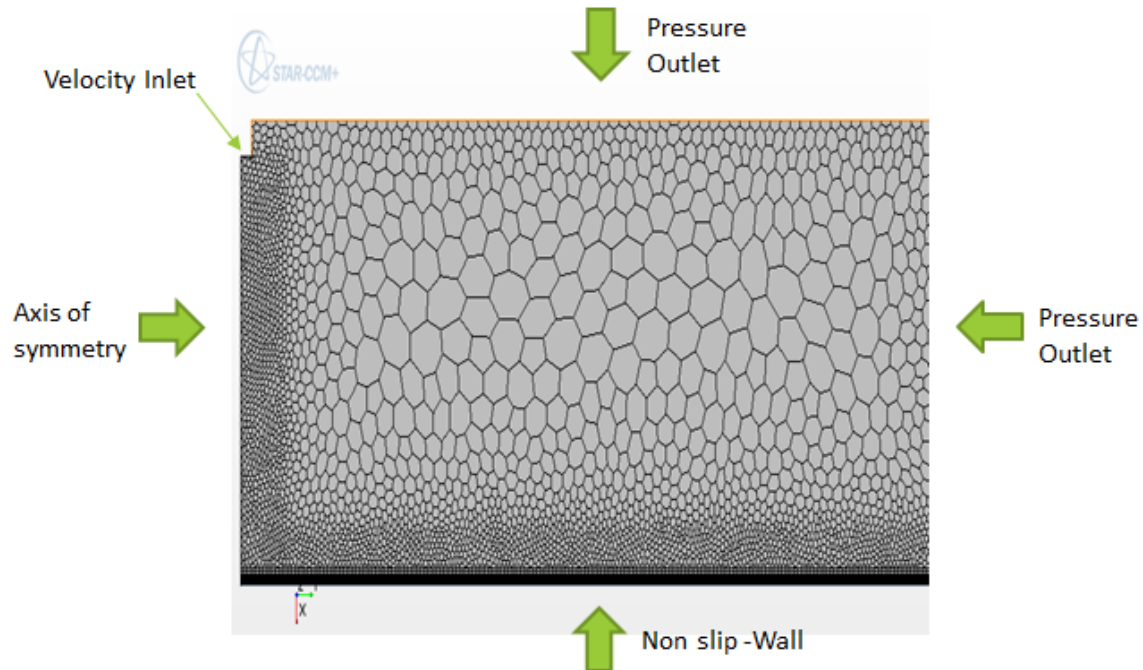


Figure 3. Full simulation domain & boundary conditions.

A velocity inlet is representing the nozzle. The impingement wall is modeled by a non-slip wall boundary condition. An axis of symmetry is placed accordingly. All other boundaries are set as pressure outlets. If the domain were to be revolved by the vertical axis, a cylindrical volume with a circular jet at the top middle would result. This accurately depicts the experimental set up laid out by Poreh's experiment.

4.2 Physics

The fluid in Poreh's experiment is air. It has a density of $.0621 \frac{lb}{ft^3}$ and a kinematic viscosity of $2 * 10^{-4} \frac{ft^2}{s} * .0621 \frac{lb}{ft^3}$. The nozzle jet velocity is $340 \frac{ft}{s}$. This velocity is in part due to what is referred to as a vena contracta. In this particular case, it results in a reduction of total area due to the inability of the fluid to instantly turn at the edges of the jet orifice diameter. This effect cannot be captured by the simulation; therefore, an effective kinematic flux is calculated as follows:

Kinematic flux in the experiment is $K = 1540 \frac{ft^4}{s^2}$. Poreh defines kinematic flux as:

$$K = \frac{\pi}{4} D^2 U_o^2$$

Equation 3. Porehs Kinematic Flux Definition

It follows that

$$U_o = \sqrt{\frac{K}{.153\pi D^2}} = \sqrt{\frac{1540 * 4}{\pi * .166^2}} = 265 \frac{ft}{s}$$

This effective velocity is the one that will be used in the simulation. The inlet will be further described by specifying a turbulent intensity as well as a turbulent length scale. The length scale will be based off of the radius of the jet, 1 inch. The turbulent intensity is then decided by an accepted inlet intensity equation for turbulent pipe flow:

$$I = .016(R_e)^{-\frac{1}{8}}$$

Equation 4. Inlet Intensity for Turbulent Pipe Flow

$$= .016(1.96 * 10^5)^{-\frac{1}{8}} = 3\%$$

Table 2 summarizes the physics models used in StarCCM+.

Table 2. Physics Modeling Summary

| Physics Model | Justification |
|--|--|
| Axisymmetric | Poreh experimentally determined that the velocity profile was axisymmetric about the center of impingement |
| Gas | Fluid under consideration is air |
| Constant Density | No significant temperature or pressure changes to affect density |
| Turbulent | Reynolds number of 1.96×10^5 |
| RANS | Computationally efficient, expected behavior is known |
| Realizable K-Epsilon | Realizable RANS model is known to have improved spreading rate of round jets |
| Segregated Flow | Low mach number and pressure, computationally efficient |
| Steady | Steady state results are of interest |
| Two-Layer All Y+ Wall Treatment | Meshing refinement zones will be best resolved by an all Y+ treatment |
| Segregated Fluid Isothermal | Temperature changes are negligible |

4.3 Mesh

The initial meshing strategy will have two different refinement zones within the entire 2D domain. The mesh will be refined in the expected projected jet area. The mesh will be coarser everywhere else where there are little expected fluctuations. The following figure illustrates the location of the jet zones.

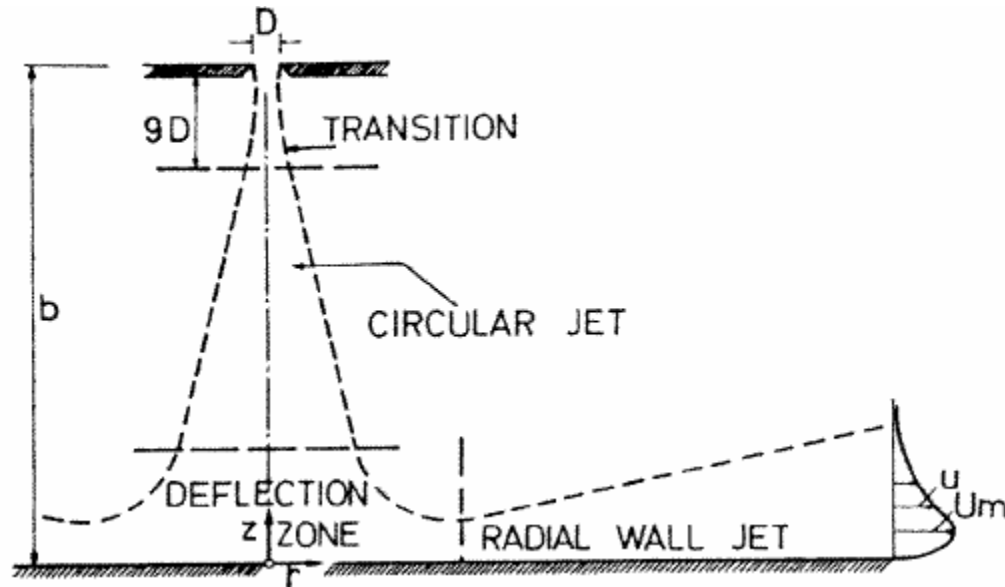


Figure 4. Jet zones (Poreh et al.)

The maximum thickness of the radial jet is set as the thickness of the refinement zone. An offset-layer is created at the impingement wall and is reduced in size in order to capture the velocity fluctuations near the wall. After some trial and error, the resulting mesh is as in the following figure.

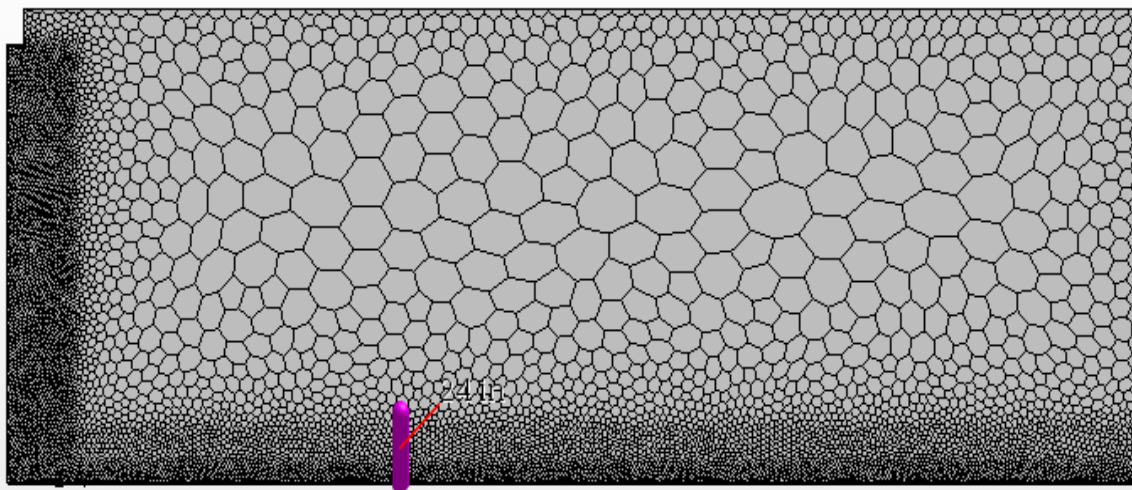


Figure 5. Final mesh.

As described, there are two meshing refinement zones. One extra refinement zone is created at the impingement wall in order to capture the sharp velocity gradients near the wall. Although not visible, a prism layer exists at the impingement plate about a millimeter thick. The following table summarizes the mesh characteristics.

Table 3. Mesh Summary

| Section | | Count |
|--|-----------------------|-----------------------|
| Base size | | 1 in. |
| Circular & Inner Radial Jet | | .2 in. |
| outer Radial jet | | .3 in. |
| Prism Layer Thickness | | .05 in. |
| layers | | 5 |
| Growth rate | | 1.3 |
| Total Mesh Count | | |
| # Cells: 10706 | # Faces: 29796 | # Verts: 19672 |

In order to validate the final mesh from which the results will be analyzed, mesh sensitivity analysis needs to be performed. This confirms that the results do not change with increasing or decreasing mesh size, leaving the solution independent of the mesh.

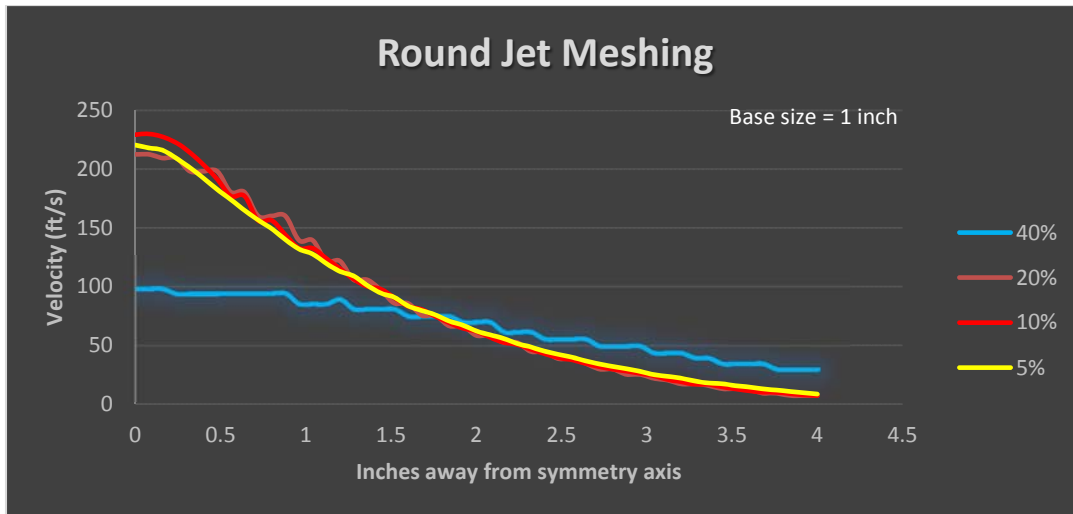


Figure 6. Round jet velocity profile (24 inches away from the nozzle).

The above figure shows how the velocity of the round jet fluctuates with distance from the axis of symmetry. We can see that at 40% of the base mesh size, the round jet does not reach maximum velocity. Furthermore, it is observed that at 20% of the base mesh size, the fluctuation in resulting velocity does not change significantly with increasing and decreasing mesh size. 20% is used for computational efficiency instead of 10%.

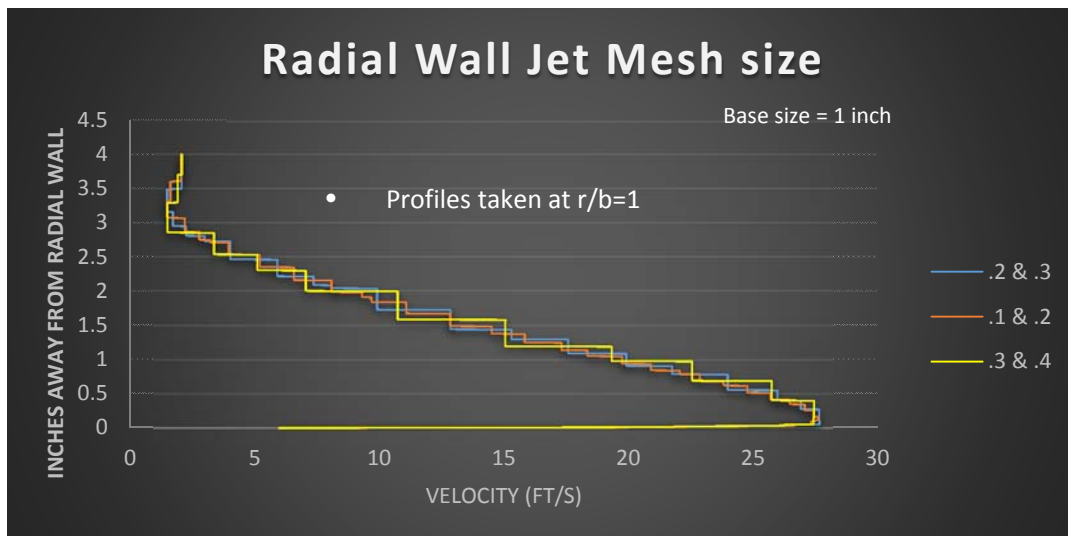


Figure 7. Radial wall jet profile (24 inches away from the axis of symmetry).

Similarly, the same analysis is done for the radial wall jet velocity profile. The radial wall jet consists of two refinement areas and therefore has two different mesh sizes. The finer mesh pertains to that of the section closest to the impingement wall. That mesh zone then gradually coarsens into the next refinement zone. From the graph above, it is seen that the mesh is largely independent of the results. Data is taken 24 inches from the axis of symmetry because it was observed that this area was most sensitive to mesh changes.

4.4 Experimental vs. StarCCM+ Replication Results

Once the mesh is finalized, the results obtained from StarCCM+ are compared to those of Poreh's experimental paper. The residuals shown below indicate that the solution has converged.

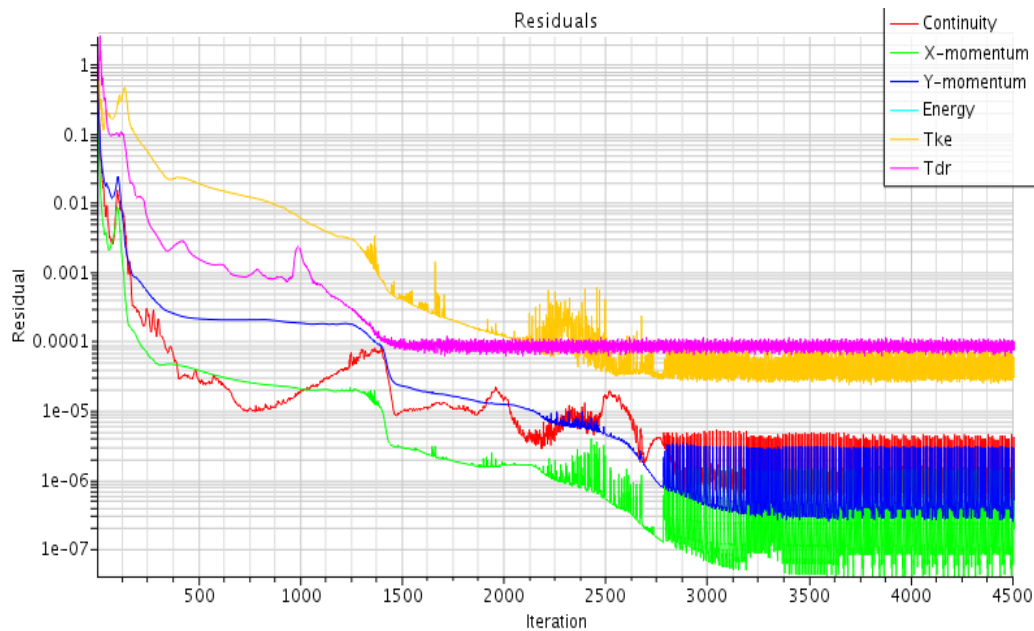


Figure 8. Residuals for StarCCM+ $b/D=12$.

Below is the magnitude velocity profile domain for $b/D=12$.

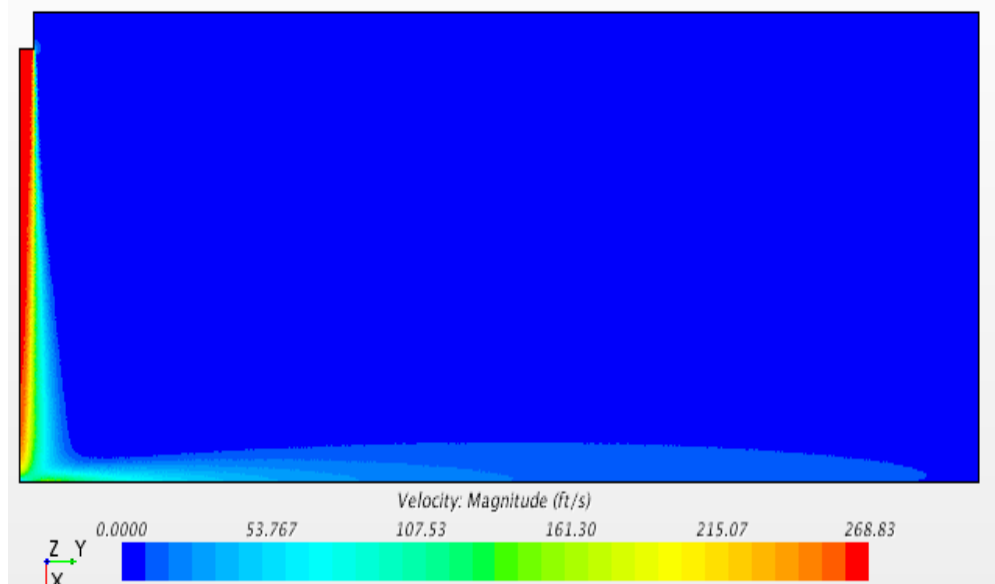


Figure 9. Velocity profile of the entire domain ($b/D=12$).

The expected behavior is observed. The round jet creates shear between the surrounding stagnant air, therefore widening the radius of the jet as it approaches the impingement surface. After

impingement, the radial wall jet is created and the thickness of the jet is increased in a similar fashion as that of the round jet.

The following graphs will compare the velocity profiles of the radial wall jet from Poreh's experiment to that of StarCCM+'s results at the different radial locations.

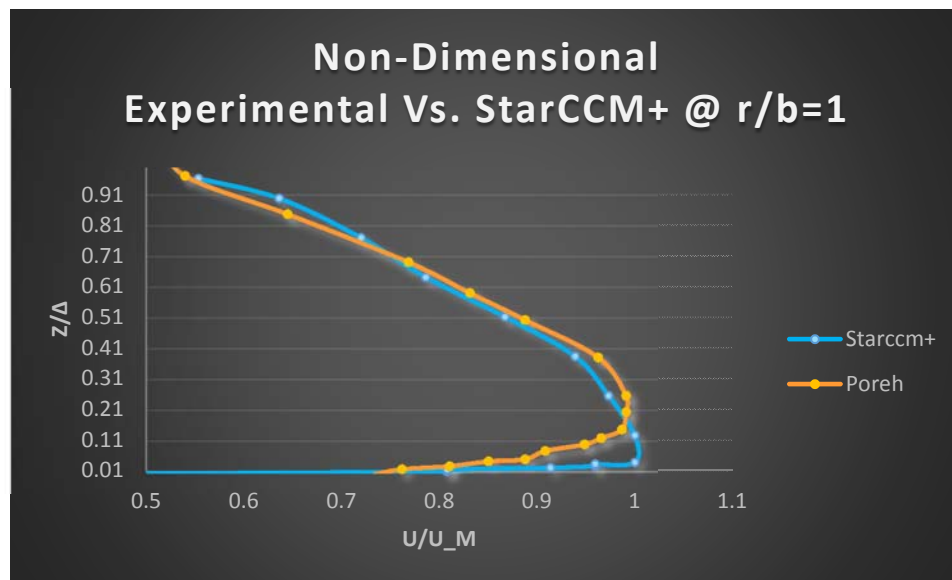


Figure 10. Non-dimensional comparison of at $r=24$ in. ($b/D=12$).

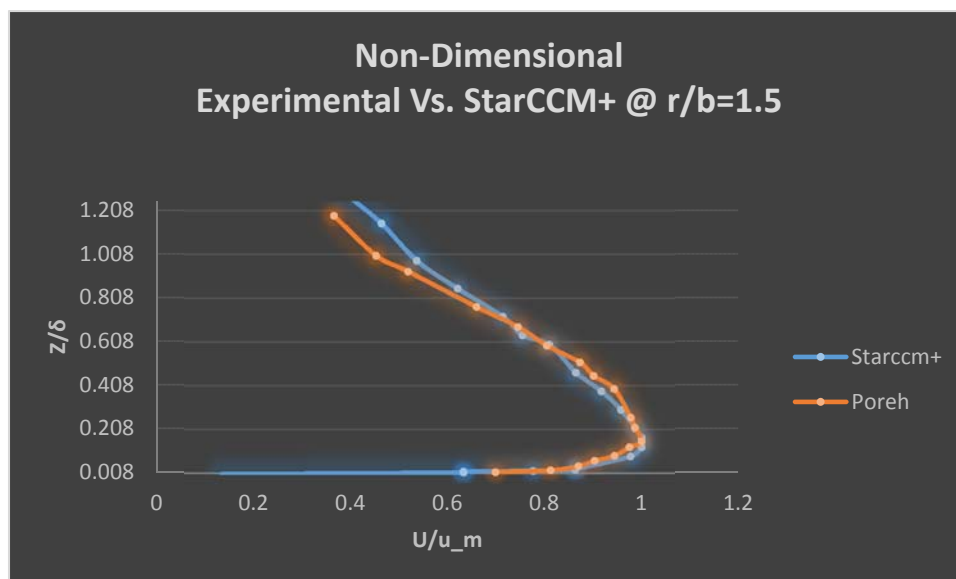


Figure 11. Non-dimensional comparison of at $r=36$ in. ($b/D=12$).

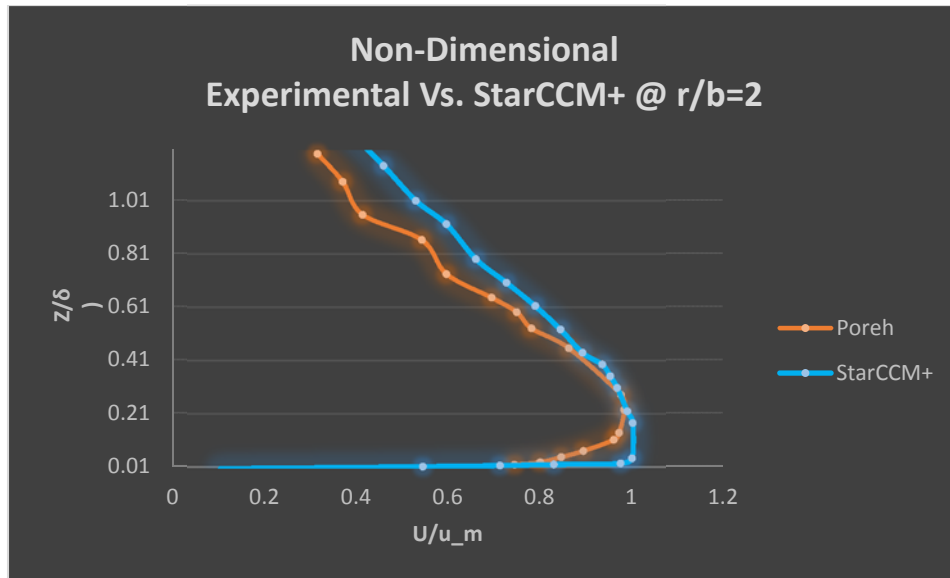


Figure 12. Non-dimensional comparison of at $r=48$ in. ($b/D=12$).

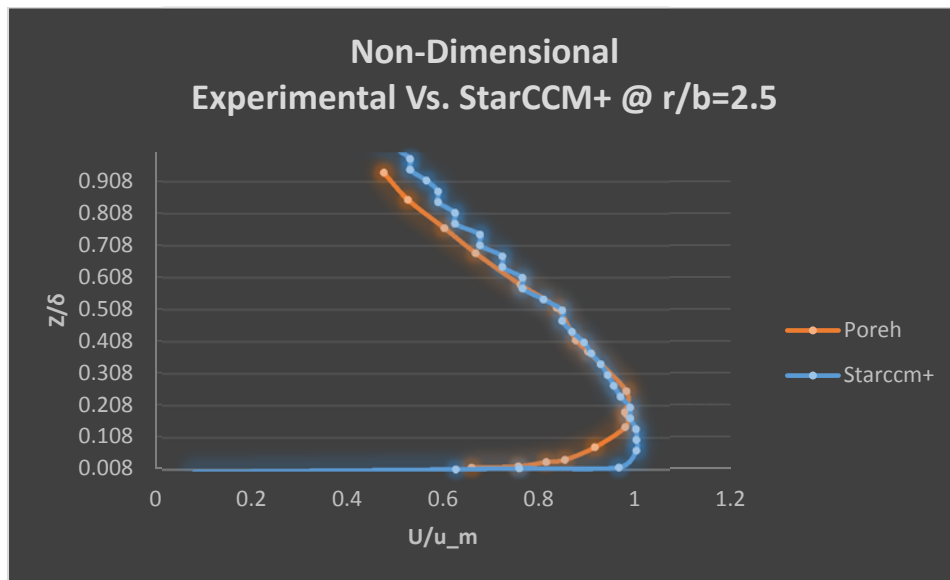


Figure 13. Non-dimensional comparison of at $r=60$ in. ($b/D=12$).

It can be seen from all the plots of the radial wall jet velocity profile comparison that the simulation agrees well with the experimental results. It is observed that the experimental results take a longer distance, as measured from the impingement wall, to reach maximum velocity. This can possibly be attributed to the fact that the probes with which the experimental data was taken might have been intrusive in nature. Regardless, the simulation results agree well with the experimental data.

5. RESULTS AND ANALYSIS

Once Poreh's experimental results were matched sufficiently well, the distance of the nozzle to the impingement plate was lowered to a b/D ratio of 1.5. The b/D ratio was the only change to the entire simulation including the physics and geometric domain. The velocity profile domain in the following figure was the result.



Figure 14. Domain velocity profile for $b/D=1.5$.

It can be seen that the nature of the velocity profile in the entire domain does not change significantly in magnitude. It is important to notice that the round jet is not given enough time to widen like in the previous case, and resembles a plug flow instead of a fully developed flow.

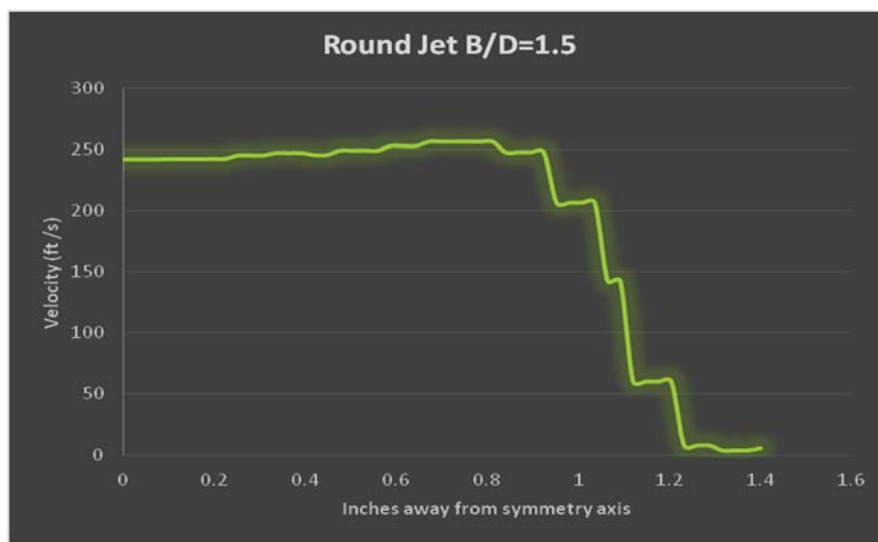


Figure 15. Velocity profile prior to impingement.

Above is a graph of the velocity profile of the round jet right before the impingement regime. It shows that the profile closely resemble that of a plug flow. Mesh sensitivity is again performed in order to assess the dependency of the results to that of the mesh.

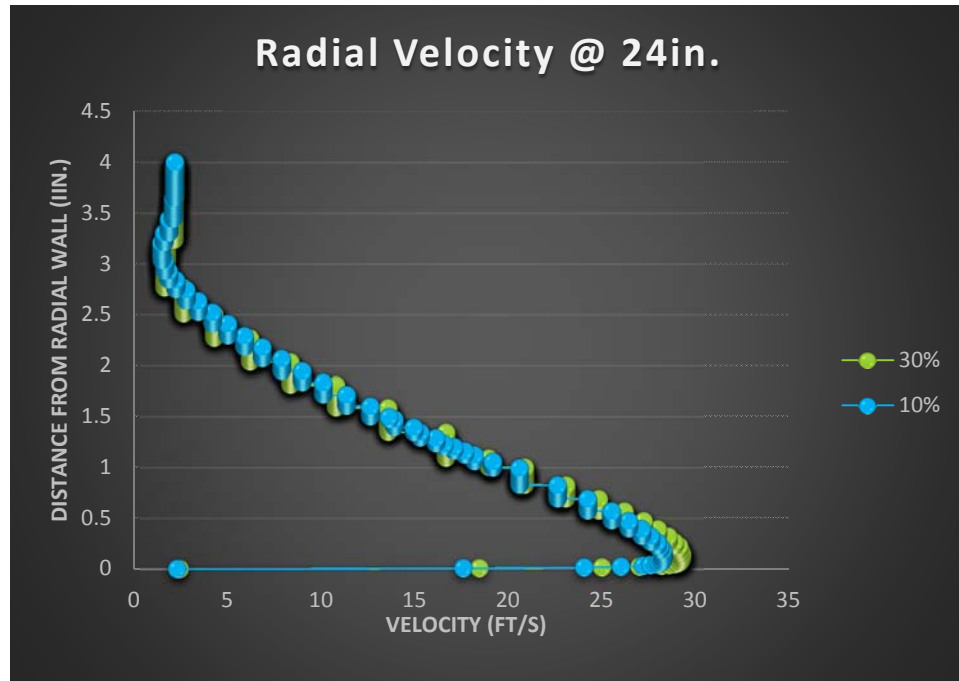


Figure 16. Mesh sensitivity for radial wall jet $b/D=1.5$.

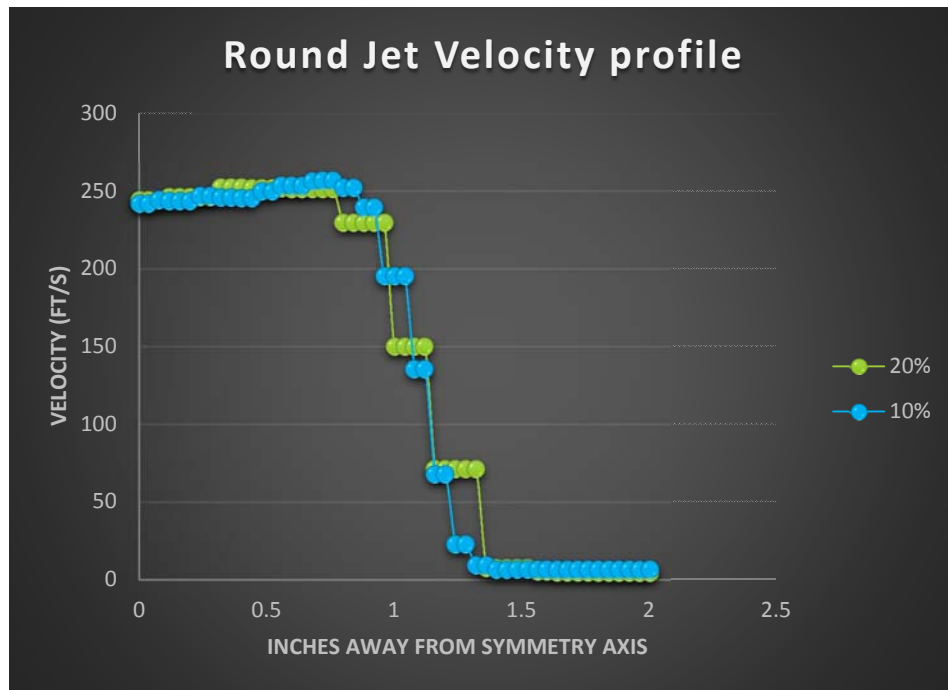


Figure 17. Mesh sensitivity pre-impingement.

From the above graphs, it is concluded that the initial mesh is sufficiently fine to continue with the analysis. The non-dimensional velocity profiles are then compared to the experimental data by Poreh. It is important to note that it is no longer appropriate to non-dimensionalize the radial location by b . An r/b ratio of one in the new study will result in being 3 inches away from the axis of symmetry, which is well within the impingement domain. Poreh's correlations were made for the radial wall jet and therefore will not be valid within the impingement zone. In an attempt to resolve this, the radial distance will be non-dimensionalized by the diameter of the nozzle and the locations looked at will be the same as those measured by Poreh's experiment. The following graphs will show how U_m and δ obtained from both simulations relate to the empirical correlations developed by Poreh.

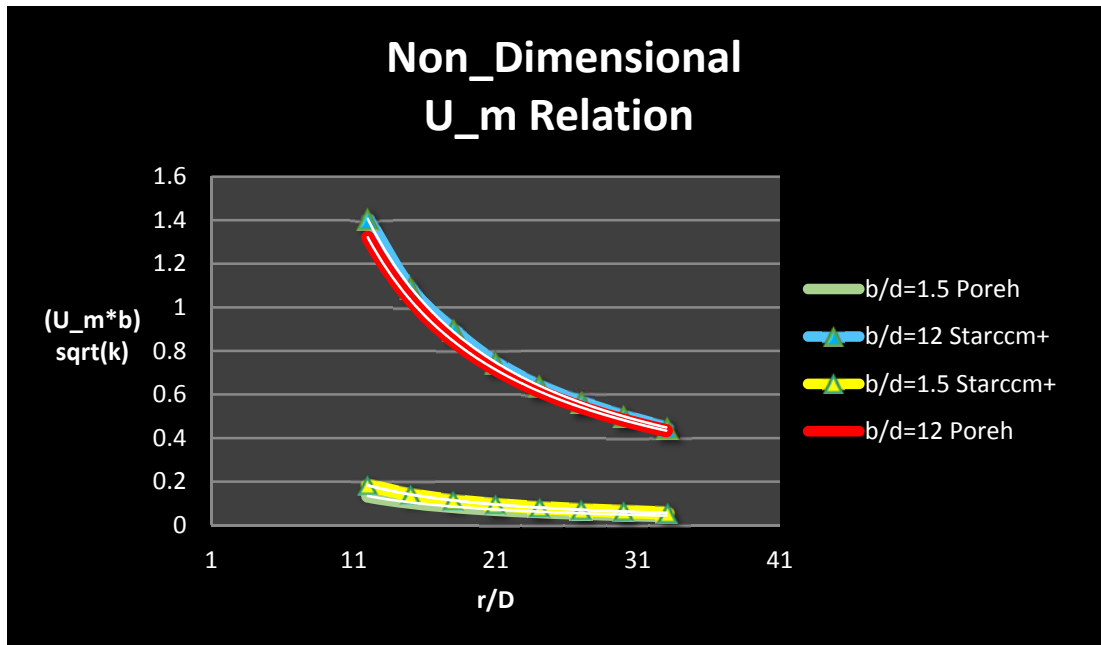


Figure 18. Non-dimensional maximum velocity comparison.

$$\text{StarCCM+ @ } b/D=12$$

$$y = 23.25x^{-1.129}$$

$$\text{Poreh @ } b/D=12$$

$$y = 20.33x^{-1.1}$$

$$\text{StarCCM+ @ } B/D=1.5$$

$$y = 3.34x^{-1.169}$$

$$\text{Poreh @ } B/D=1.5$$

$$y = 2.06x^{-1.1}$$

It seems as though the correlation matches for both b/D cases. Using b/D of 1.5, the equations show that the coefficient obtained from StarCCM+ is 60% higher than Poreh's correlation. The power coefficient from StarCCM+ matches well with the experimental correlation. Below is a close up of the $b/D=1.5$ comparisons.

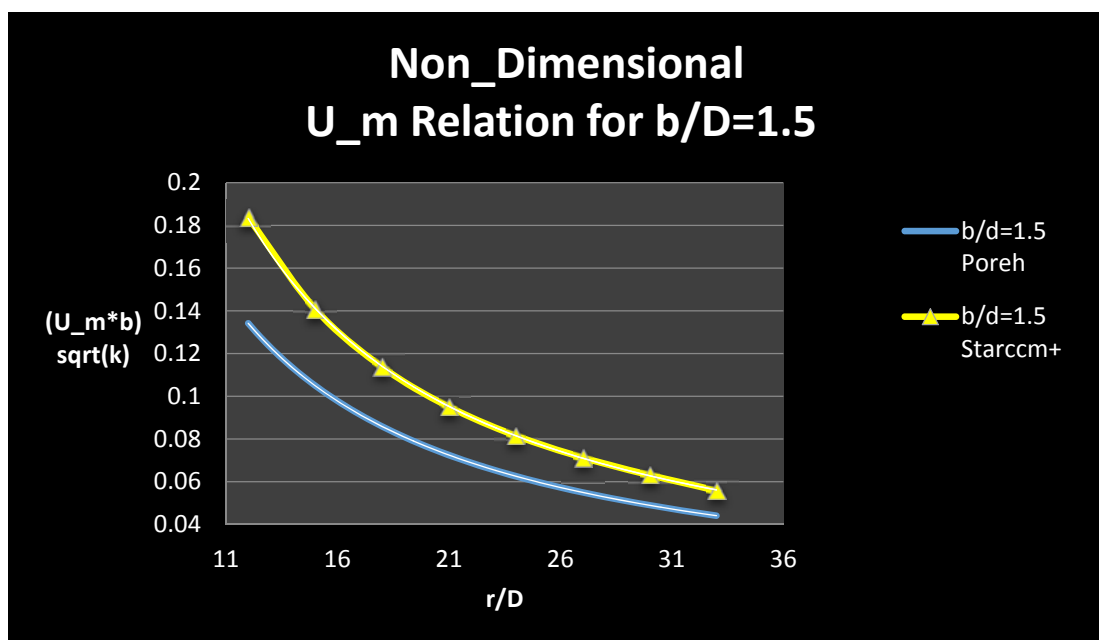


Figure 19. Close up of non-dimensional comparison.

Although there is certainly a difference, the results seem to stay within a proportional difference which is not completely misleading. The following graphs show the resulting δ comparison for both simulations.

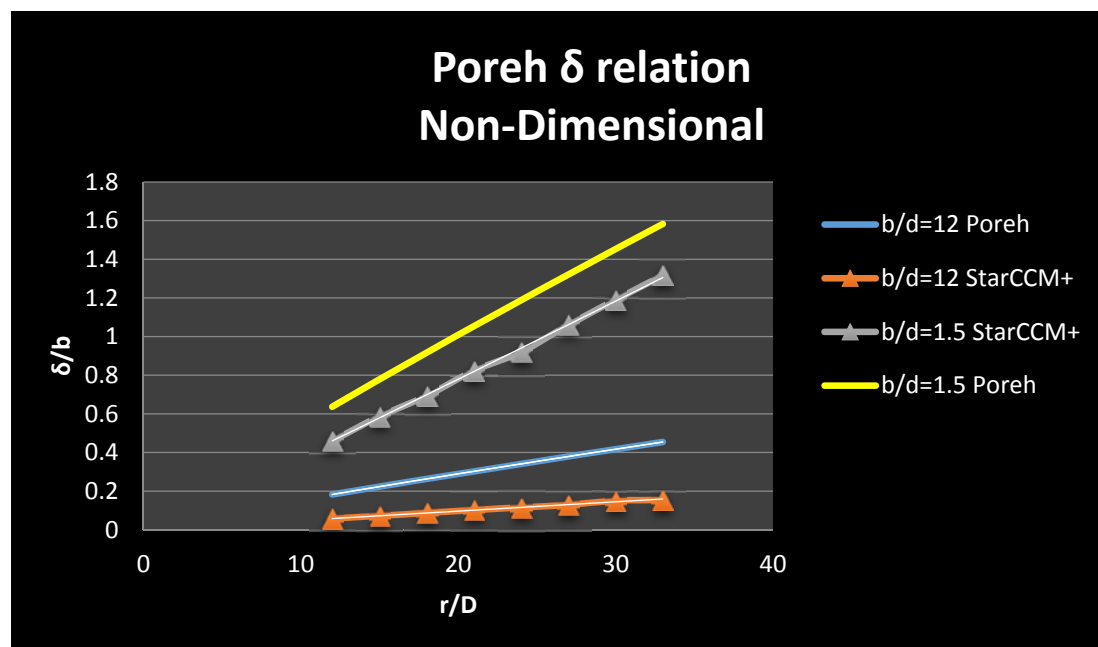


Figure 20. Non-dimensional δ correlation comparison.

$$\textbf{StarCCM+ @ B/D=12}$$

$$y = .006x^{0.9426}$$

$$\textbf{Poreh}$$

$$y = .0195x^{0.9}$$

$$\textbf{StarCCM+ @ B/D=1.5}$$

$$y = .0356x^{1.03}$$

$$\textbf{Poreh @ B/D=1.5}$$

$$y = .068x^{.9}$$

We see again a decent agreement in terms of the power coefficient for both comparisons. Although it is clearly seen that the simulation does not perfectly match the experimental correlation, it appears that the slope and magnitude of the simulation curve fittings behave in a similar fashion as the experimental data. From the curve fitting equations, the simulation predicts that the error for the maximum velocity decreases as you look farther away from impingement. The simulation also predicts that there is a slight increase in error for the δ correlation as you look further away from impingement.

6. CONCLUSION

From the results, it is concluded that the experimental correlations predicted the radial jet velocity profile characteristics with a b/D ratio of 1.5 within a reasonable range. When using such correlations, one should pay close attention to the distance from the impingement at which one is attempting to use them.

The criticism on the application of such correlations to the PJMs should lessen but not disappear. The impingement plate in the PJMs is actually at an angle. This can add gravitational effects as well as different impingement characteristics that are potentially not negligible. It is necessary that further error and geometrical analysis be performed in order to better understand the applicability of Poreh's correlation to the PJMs.

7. REFERENCES

- [1] Guenther, C.P. and Garg, R., Technical Report on NETL's Non Newtonian Multiphase Slurry Workshop: A path forward to understanding non-Newtonian multiphase slurry flows, NETL-PUB-926, NETL Technical Report Series, U.S. Department of Energy, National Energy Technology Laboratory. OSTI ID: 1121879.
- [2] Poreh, M., Tsuei, Y., & Cermak, J. (1967). Investigation of a Turbulent Radial Wall Jet. *Journal of Applied Mechanics J. Appl. Mech.*, 457-457.